

## Mechanisms of the Wurtzite to Rocksalt Transformation in CdSe Nanocrystals

Michael Grünwald,<sup>1</sup> Eran Rabani,<sup>2</sup> and Christoph Dellago<sup>1</sup>

<sup>1</sup>Faculty of Physics and Center for Computational Materials Science, University of Vienna, Boltzmannngasse 5, 1090 Vienna, Austria

<sup>2</sup>School of Chemistry, Tel Aviv University, Tel Aviv 69978, Israel

(Received 7 March 2006; published 27 June 2006)

We study the pressure-driven phase transition from the four-coordinate wurtzite to the six-coordinate rocksalt structure in CdSe nanocrystals with molecular dynamics computer simulations. With an ideal gas as the pressure medium, we apply hydrostatic pressure to spherical and faceted nanocrystals ranging in diameter from 25 to 62 Å. In spherical crystals, the main mechanism of the transformation involves the sliding of (100) planes, but depending on the specific surface structure we also observe a second mechanism proceeding through the flattening of (100) planes. In faceted crystals, the transition proceeds via a five-coordinated hexagonal structure, which is stabilized at intermediate pressures due to dominant surface energetics.

DOI: 10.1103/PhysRevLett.96.255701

PACS numbers: 64.70.Nd, 61.46.Df, 71.15.Pd

The thermodynamic properties of nanosized particles can differ significantly from those of the corresponding bulk materials due to the large surface to volume ratio. In particular, the kinetics and the mechanism of first order phase transitions are strongly affected by the surface free energetics of such systems. In a series of recent experiments, Alivisatos and co-workers [1–6] have demonstrated that the pressure-induced transition from the four-coordinate wurtzite structure to the six-coordinate rocksalt structure in CdSe is strongly influenced by crystal size. The transition pressure increases by about a factor of 2 as the size of the sample is decreased from macroscopic dimensions to the nanometer scale [1], and also the kinetics of this highly activated process change markedly as a function of size [2,4].

A considerable amount of work has been concerned with the wurtzite to rocksalt transition and possible intermediate structures in the bulk [7–15] where, for CdSe, the transformation occurs at approximately 2.5 GPa [16,17]. In a recent molecular dynamics study of bulk CdSe, Shimojo *et al.* identified two main mechanisms [12]. The first mechanism was previously proposed by Tolbert and Alivisatos and involves the flattening out of parallel (100) planes [1], the second mechanism is realized through sliding of parallel (100) planes along the [010] direction. Using transition path sampling methods [18], Zahn, Grin, and Leoni recently showed that the second mechanism is highly preferred and the transition does not involve a concerted motion of atoms, but occurs via nucleation and growth [15].

In the nanocrystal, surface effects may significantly alter the transition mechanism. In this Letter, we use molecular dynamics simulation to study the structural transformation of CdSe nanocrystals of various shapes and sizes. Our simulations reveal that transition mechanisms are strongly shape dependent: Most *spherical* nanocrystals transform through the bulk mechanism of sliding (100) planes [15], but the other mechanism, unfavored in the bulk, also occurs. For *faceted* nanocrystals the transformation pro-

ceeds through an intermediate five-coordinate structure, that is unstable in the bulk but is stabilized by surface effects in the nanoparticle.

In all our simulations we use the empirical pair potential for CdSe developed by Rabani [17], designed to reproduce the lattice and elastic constants of bulk CdSe as well as the bulk wurtzite to rocksalt transition pressure of 2.5 GPa [15,17].

A crucial point in the simulation of nanoparticles under pressure is the choice of pressure medium. As such we use an ideal gas of noninteracting particles that interact with the crystal atoms through the soft-sphere pair potential  $u(r) = \epsilon(\sigma/r)^{12}$ . As the equation of state of the ideal gas is known analytically, the pressure can be easily tuned by controlling the density of the pressure bath. We set  $\epsilon = 1$  kJ/mol and  $\sigma = 3.0$  Å, large enough to prevent infiltration of gas particles into the nanocrystal. For an efficient calculation of the forces needed in the molecular dynamics simulation, we use cell lists [19] and a cutoff of  $2\sigma$  for the interactions between ideal gas particles and the crystal atoms. To reduce the number of ideal gas particles required to exert a given pressure, these particles fill only a thin layer around the crystal. The volume that is occupied by the gas consists of all cells, already defined for the cell lists, that can hold possible interaction partners of the crystal atoms. This minimal volume of cells is updated every time step and particles leaving the volume are no longer considered. The loss of gas particles is compensated by randomly introducing new gas particles on the cell walls confining the volume, with statistics appropriate for an ideal gas at temperature  $T$  and pressure  $P$ . When, by movement of crystal atoms, a new cell is added to the gas atmosphere, it is filled with a number of particles drawn from an appropriate Poisson distribution; when a cell is removed from the gas atmosphere, the particles in this cell are no longer considered. In this method, the gas serves as a barostat as well as a thermostat. The exerted pressure is hydrostatic (we have numerically verified that in our simulations the forces tangential to the crystal

surfaces vanish on average) and can be simply controlled by adjusting the number of ideal gas particles.

To study the effect of surface structure and crystal size on the transition mechanism, we use nanocrystals of two different shapes, ranging in radius from 12.6 to 31.5 Å, consisting of 300 to 4500 atoms. Spherical nanocrystals are cut from a large wurtzite lattice with centers randomly distributed over the wurtzite unit cell. The resulting nanocrystals have disordered surfaces and, due to the randomly chosen positions of the center, slightly differ in atom number even for equal sizes. Faceted nanocrystals with well-defined surface structure were obtained by cleaving the bulk lattice along equivalent (100) wurtzite planes and at (001) and (00 $\bar{1}$ ) planes perpendicular to the [001] direction of the  $c$  axis. Similar to crystals used in experiments [20], the aspect ratio was chosen to vary around a value of 1.25, slightly elongated along the  $c$  axis. The resulting nanocrystals have stable low-index surfaces and can be seen as a short version of the nanorods studied in recent experiments [6].

All of our simulations are carried out at  $T = 300$  K and follow the same scheme: A single crystal is initially equilibrated for 15 ps at zero pressure. Then the pressure is increased every 10 ps in steps of 0.25 GPa until a maximum pressure of 8–11 GPa is reached, depending on crystal size and shape. The equations of motion are integrated using the velocity Verlet algorithm [21] with a time step of 2 fs. The mass of the ideal gas particles is 10 amu. The longest of a total of 75 simulation runs have a length of 450 ps, and about 350 000 gas particles are required to apply a maximum pressure of 11 GPa.

Apart from analyzing the simulation runs by visual inspection, we calculate the number of atoms  $N_i$  with  $i$  nearest neighbors. Here, atoms are defined to be nearest

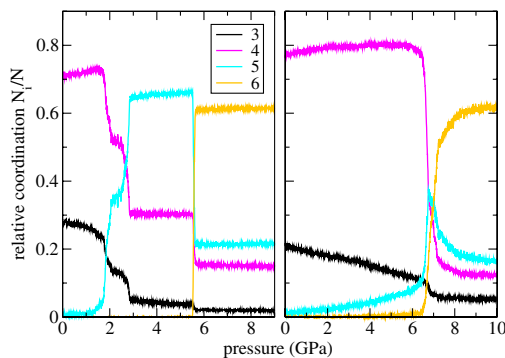


FIG. 1 (color online). Relative coordination  $N_i/N$  as a function of pressure for a *faceted*  $\text{Cd}_{847}\text{Se}_{847}$  crystal (left) and a *spherical*  $\text{Cd}_{1456}\text{Se}_{1457}$  crystal (right). The wurtzite to rocksalt transition can be easily identified through the change from predominant four-coordination to six-coordination. In faceted crystals (left), the stable five-coordinated  $h$ -MgO structure is observed at intermediate pressures. For spherical crystal shapes (right), the transformation from four-coordination to six-coordination occurs directly and the intermediate  $h$ -MgO structure is never observed.

neighbors if they are closer than 3.3 Å, the location of the first minimum of the radial distribution function. The transition is monitored by plotting the fractions  $N_i/N$  of  $i$ -coordinated atoms as a function of pressure (see Fig. 1). Whereas spherical crystals directly transform from the wurtzite to the rocksalt structure, as indicated by the sudden change from four- to six-coordination (Fig. 1, right), faceted crystals take a five-coordinated structure at intermediate pressures (Fig. 1, left). The latter transition is depicted in Fig. 2(a). Starting on one side of the crystal, the puckered wurtzite (001) layers are leveled out, leading to a compression of the whole crystal along the wurtzite  $c$  axis. The resulting structure is similar to hexagonal BN and was named  $h$ -MgO, as it was first discovered as a metastable phase of MgO [8]. Recently, it was considered as a metastable intermediate in the wurtzite to rocksalt transition in bulk CdSe [12]. Its high energy, however, rules it out as a possible stable intermediate structure for the bulk transformation [12]. To confirm this, we calculate the enthalpy of bulk CdSe in constant-pressure Monte Carlo simulations (see Fig. 3) [17]. The enthalpy of  $h$ -MgO is never the lowest, rendering this structure unaccessible in the bulk. During the transition, the (001) planes of the crystal are flattened out and the surface atoms are shifted from a three-coordinate to a four-coordinate environment.

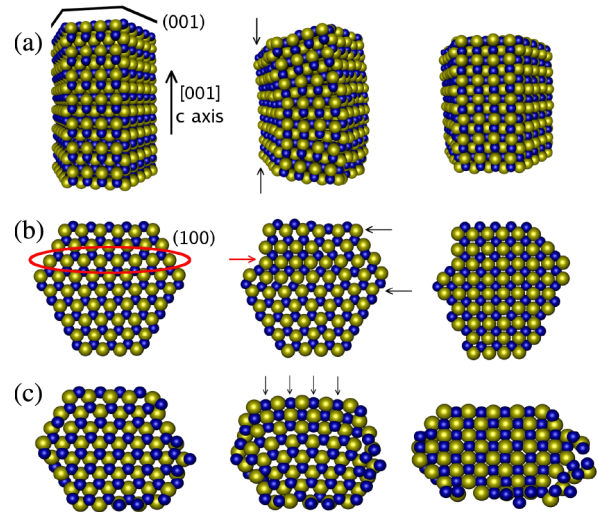


FIG. 2 (color online). (a) Wurtzite to  $h$ -MgO transition mechanism in a *faceted*  $\text{Cd}_{847}\text{Se}_{847}$  crystal. The transition occurs through a compression of the crystal in the direction of the wurtzite  $c$  axis, the puckered (001) layers, indicated in the figure, are flattened out. (b)  $h$ -MgO to rocksalt transition mechanism in a *faceted*  $\text{Cd}_{847}\text{Se}_{847}$  crystal, seen down the wurtzite  $c$  axis. The transition starts on the surface with the displacement of the outer atoms of a (100) plane into the crystal (red arrow), forming the rocksalt nucleus. Next-nearest neighbor planes preferably slide in alternate directions (black arrows). (c) Wurtzite to rocksalt transition mechanism in a *spherical*  $\text{Cd}_{366}\text{Se}_{359}$  crystal, seen down the wurtzite  $c$  axis. Starting on the surface, atoms across six-membered hexagonal rings come together to form the rocksalt structure, flattening out the wurtzite (100) planes.

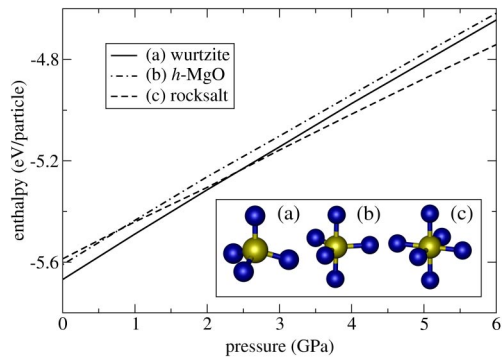


FIG. 3 (color online). Enthalpy as a function of pressure for bulk CdSe in the wurtzite,  $h$ -MgO and rocksalt structure obtained from Monte Carlo simulations at constant pressure and temperature. Inset: Atomic configuration for the three structures.

This favorable reorganization of the surface stabilizes the five-coordinate  $h$ -MgO structure in the nanocrystal sufficiently with respect to the bulk to make this structure accessible during the transition. As expected, we observe a strong decrease in the wurtzite to  $h$ -MgO transition pressure with decreasing crystal size [22]: Whereas in the largest crystals the  $h$ -MgO structure is stable over a small pressure range only, we observe an immediate wurtzite to  $h$ -MgO transition at zero pressure for a  $\text{Cd}_{72}\text{Se}_{72}$  crystal. The critical size, at which the  $h$ -MgO structure becomes unstable with respect to the wurtzite structure, increases with increasing pressure.

The  $h$ -MgO to rocksalt transition is shown in Fig. 2(b). The mechanism involves the sliding of parallel (100) planes and is equal to the mechanism observed in the bulk [15], except for the compression along the wurtzite  $c$  axis, which has already occurred during the wurtzite to  $h$ -MgO transition. The transition nucleates at the surface where the outer atoms of a (100) plane move along the [010] direction into the crystal, transforming the hexagonal  $120^\circ$  bond angle along the (100) plane into the cubic  $90^\circ$  angle. Cadmium and selenium atoms along the plane form cubic bonds with the next selenium and cadmium atoms along the two neighboring (100) planes, initiating the rocksalt nucleus. This displacement and change of angle quickly propagates along the (100) plane, at the same time starting the transition in the adjacent (100) planes. This sliding plane motion then moves through the whole crystal. The shearing directions of the planes, parallel or antiparallel, vary and determine the overall shape change of the crystal during the transformation. In some of the larger faceted crystals, we observe the formation of grain boundaries during the  $h$ -MgO to rocksalt phase transition. If the crystal is sufficiently large, the transition can occur in different parts of the crystal simultaneously. Grain boundaries then form where two rocksalt structures with different orientation meet.

The majority of spherical crystals transforms through the sliding of (100) planes mechanism observed in the  $h$ -MgO to rocksalt transition of faceted crystals. How-

ever, the transition occurs directly from the wurtzite to the rocksalt structure and the  $h$ -MgO structure is not observed. The compression of the wurtzite lattice in the direction of the  $c$  axis takes place at the same time as the shearing motion of (100) planes. In faceted crystals with flat (001) surfaces terminating the crystal in the  $c$  direction, there is no transition motion in the [001] direction during the  $h$ -MgO to rocksalt transition, leading to a flat, low-index (001) rocksalt surface. The situation is different in spherical crystals. As the spherical shape is not suitable to accommodate low-index rocksalt faces, the transition motion is more complicated. In an effort to produce low-energy rocksalt surfaces, wurtzite (100) planes can, in addition to the shearing motion, move in the [001] direction during the transition. Moreover, the formation of lattice defects is found in spherical crystals of all sizes. These include grain boundaries between rocksalt domains of different orientation, as well as dislocations. Whereas only one  $14 \text{ \AA}$  crystal displays a grain boundary after the transition, over 80% of the largest sized crystals transform with lattice defects.

In a single, spherical  $\text{Cd}_{366}\text{Se}_{359}$  nanocrystal we observed a second transition mechanism [Fig. 2(c)]. Here, the transition does not involve a shearing motion but a flattening out of (100) planes. Starting on one side of the crystal, atoms across six-membered hexagonal rings come together to form the rocksalt structure and at the same time level differences in the  $c$  direction are flattened out. A transition through this mechanism requires a significant overall shape change of the crystal, transforming a sphere into an oblate ellipsoid. This mechanism was previously proposed and later discarded by Alivisatos *et al.* [1,3], because the significant shape change accompanying the transition through this mechanism could not be confirmed by experimental data [3]. The exact prerequisites for the two different mechanisms to happen are unclear, but seem to be strongly dependent on the specific surface structure. Although we observe the alternative mechanism in this pureness only in one case, many  $14.0 \text{ \AA}$  radius crystals and even a few larger crystals, spherical and faceted, display a mixture of both mechanisms.

While our simulations show many similarities with actual experiments on CdSe nanocrystals, there are also important differences. The  $h$ -MgO structure is not observed in experiments and the transition mechanism proposed in agreement with experimental data involves the sliding of (001) planes [3], not (100) planes as in our simulations. However, a possibly metastable  $h$ -MgO structure might have a lifetime too short to be resolved in the experiments. Also, crystals used in experiments are covered with surfactants, which strongly influence surface energies [23]. The presence of such a surface passivation layer may block the transition path to the  $h$ -MgO structure and render it inaccessible in the experiments, favoring a different transition mechanism. Computationally quite a challenge, a detailed description of surface passivation nevertheless has to be included in future simulations.

Recently, progress has been made towards a description of surfactants through simple force fields [24].

Another difference between simulation and experiment lies in the accessible time scales. Although our rate of pressurization is lower than in comparable simulation studies [25–29], it is still many orders of magnitude larger than in experiments, where observation times of several minutes up to hours are common [3]. This has two effects: First, sudden changes in pressure can lead to structural instabilities, possibly changing the statistical weight of different transition mechanisms. Second, on the short time scale available in simulations, the use of significantly higher pressures is necessary to observe the transition. This again may lead to different transition mechanisms. Despite the large difference in time scale, the transitions in our simulations happen at pressures comparable to those found in experiments. This indicates that transition barriers are quite different in the two cases, again pointing to the important role of surface passivation. To study the transition at the thermodynamic transition pressure, transition path sampling methods will be applied in future work [15,18].

The observation of grain boundaries in our simulations is another striking difference to the experiments, where nanocrystals transform free of defects over many pressure cycles [1,4]. The main mechanism in the formation of these defects is surface related: When the simple sliding-planes motion would introduce too many surface defects in the final rocksalt structure, as in the case of the spherical crystals, different domains of rocksalt are formed to minimize the surface free energy by the formation of low-index rocksalt surfaces. In faceted crystals, the sliding-planes motion alone leads to well-defined rocksalt surfaces. The formation of lattice defects in this case would destroy these surfaces, introducing high-energy steps and edges. Nevertheless, grain boundaries can form in faceted crystals if, due to the high degree of over pressurization, the transformation is triggered in different parts of the crystal simultaneously. Recently, a simulation study of GaAs nanocrystals showed results similar to our work [25,26]: Larger spherical crystals are found to transform with grain boundaries, whereas faceted crystals more often display single-domain behavior.

In conclusion, we show that the structural transformation in CdSe nanocrystals is dominated by surface effects. The transformation nucleates at the surface and proceeds via the bulk mechanism of sliding (100) planes, but depending on the details of the surface structure, other mechanisms involving the flattening of (100) planes or the formation of a five-coordinate intermediate structure are possible. Moreover, our simulations show that in nanocrystals it is possible to stabilize structures that are unstable in the bulk by controlling the overall shape and surface structure of the particles.

This work was supported by the Austrian Science Fund (FWF) within the Science College “Computational Materials Science” under Grant No. W004.

- [1] S.H. Tolbert and A.P. Alivisatos, *J. Chem. Phys.* **102**, 4642 (1995).
- [2] C.-C. Chen, A.B. Herhold, C.S. Johnson, and A.P. Alivisatos, *Science* **276**, 398 (1997).
- [3] J.N. Wickham, A.B. Herhold, and A.P. Alivisatos, *Phys. Rev. Lett.* **84**, 923 (2000).
- [4] K. Jacobs, D. Zaziski, E. C. Scher, A. B. Herhold, and A. P. Alivisatos, *Science* **293**, 1803 (2001).
- [5] K. Jacobs, J. Wickham, and A.P. Alivisatos, *J. Phys. Chem. B* **106**, 3759 (2002).
- [6] D. Zaziski, S. Prilliman, E.C. Scher, M. Casula, J. Wickham, S.M. Clark, and A.P. Alivisatos, *Nano Lett.* **4**, 943 (2004).
- [7] M.D. Knudson, Y.M. Gupta, and A.B. Kunz, *Phys. Rev. B* **59**, 11 704 (1999).
- [8] S. Limpijumnong and W.R.L. Lambrecht, *Phys. Rev. Lett.* **86**, 91 (2001).
- [9] S. Limpijumnong and W.R.L. Lambrecht, *Phys. Rev. B* **63**, 104103 (2001).
- [10] S. Limpijumnong and S. Jungthawan, *Phys. Rev. B* **70**, 054104 (2004).
- [11] M. Wilson and P. A. Madden, *J. Phys. Condens. Matter* **14**, 4629 (2002).
- [12] F. Shimojo, S. Kodiyalam, I. Ebbsjö, R.K. Kalia, A. Nakano, and P. Vashishta, *Phys. Rev. B* **70**, 184111 (2004).
- [13] H. Sowa, *Acta Crystallogr. Sect. A* **57**, 176 (2001).
- [14] H. Sowa, *Acta Crystallogr. Sect. A* **61**, 325 (2005).
- [15] D. Zahn, Y. Grin, and S. Leoni, *Phys. Rev. B* **72**, 064110 (2005).
- [16] H. Sowa, *Solid State Sci.* **7**, 1384 (2005).
- [17] E. Rabani, *J. Chem. Phys.* **116**, 258 (2002).
- [18] C. Dellago, P.G. Bolhuis, F.S. Csajka, and D. Chandler, *J. Chem. Phys.* **108**, 1964 (1998).
- [19] M.P. Allen and D.J. Tildesley, *Computer Simulation of Liquids* (Clarendon, Oxford, 1991).
- [20] J.J. Shiang, A.V. Kadavanich, R.K. Grubbs, and A.P. Alivisatos, *J. Phys. Chem.* **99**, 17417 (1995).
- [21] D. Frenkel and B. Smit, *Understanding Molecular Simulation* (Academic, New York, 2002).
- [22] While the transition pressure to the intermediate *h*-MgO structure decreases with decreasing crystal size, the phase transition pressure for the overall wurtzite to rocksalt transition, obtained by averaging the upstroke and downstroke transition pressures, shows the opposite trend, as observed in the experiments.
- [23] L. Manna, L. W. Wang, R. Cingolani, and A. P. Alivisatos, *J. Phys. Chem. B* **109**, 6183 (2005).
- [24] E. Rabani, *J. Chem. Phys.* **115**, 1493 (2001).
- [25] S. Kodiyalam, R.K. Kalia, H. Kikuchi, A. Nakano, F. Shimojo, and P. Vashishta, *Phys. Rev. Lett.* **86**, 55 (2001).
- [26] S. Kodiyalam, R. K. Kalia, A. Nakano, and P. Vashishta, *Phys. Rev. Lett.* **93**, 203401 (2004).
- [27] B.J. Morgan and P.A. Madden, *Nano Lett.* **4**, 1581 (2004).
- [28] R. Martoňák, C. Molteni, and M. Parrinello, *Phys. Rev. Lett.* **84**, 682 (2000).
- [29] R. Martoňák, L. Colombo, C. Molteni, and M. Parrinello, *J. Chem. Phys.* **117**, 11 329 (2002).